13th International Symposium on Particle Image Velocimetry – ISPIV 2019
Munich, Germany, July 22-24, 2019

PIV measurement uncertainty in combustion flows due to inhomogeneous refractive index fields

Christoph Vanselow*[1], Dirk Stöbener[1], Johannes Kiefer[2], Andreas Fischer[1]

[1]University of Bremen, Institute for Metrology, Automation and Quality Science, Bremen, Germany

[2]University of Bremen, Technische Thermodynamik, Badgasteiner Str. 1, 28359 Bremen, Germany

* c.vanselow@bimaq.de

Abstract

Optical measurements inside reacting flows are often disturbed by refractive index fields, e.g. due to the strong density gradients in flames. Although occurring measurement errors due to light refraction are a known problem for certain particle image velocimetry (PIV) applications, only a qualitative analysis of the resulting measurement uncertainty inside flame flows has been carried out to date. We propose a novel experimental method providing quantitative information about occurring measurement errors inside flame flows due to refractive index fields. For this purpose, a premixed propane flame is used as an example. The uncertainty analysis is based on the determination of occurring particle position errors due to light refraction inside the flame. For three different measurement planes, the velocity field is measured with PIV and the particle position errors are experimentally determined. In the examined flow, maximal position errors amount up to 14 µm and yield significant systematic velocity errors of up to 4.5 % and random velocity errors of up to 9 %. In contrast to the systematic velocity error, the random velocity error varies significantly for the analyzed measurement planes inside the flame flow.

1 Introduction

Particle image velocimetry (PIV) provides optical measurements of flow velocity fields, which are essential for combustion diagnostics (Steinberg et al., 2010; Fischer, 2017). The typical PIV measurement uncertainty is about 1−2 % (Westerweel, 1997; Voges et al., 2007) and is caused, for example, by photon shot noise (Fischer, 2016) and other intensity variations of the particle images (Nobach and Bodenschatz, 2009). Especially for PIV measurements inside combustion systems, the measurement is further disturbed by inhomogeneous refractive index fields, which cause light ray deflections in the illumination path and the scattering light path from the particle to the camera. This leads to particle image distortions and, thus, to measurement errors in general.

Refractive index fields depend on the density distribution of the optical media influenced by temperature and pressure fields. In addition, for measurements inside reacting or multiphase media (e.g. flames, aerosols, and sprays), the refractive index field also depends on the distribution and condition of the individual species. As the refractive index field depends on multiple parameters, a measurement of the refractive index field itself or the resulting light refraction are often the method of choice for a quantification of the resulting PIV measurement uncertainty.

An indirect measurement of the refractive index field of a hot jet flow can be achieved by a temperature field measurement which was recently performed in (Vanselow and Fischer, 2018) using a thermocouple. The resulting PIV measurement uncertainty inside the flow was estimated by the determination of resulting particle position errors inside the flow with ray-tracing simulations. Further, the dependency of the camera perspective and the resulting triangulation error was analyzed in order to estimate resulting measurement errors also for stereoscopic and tomographic PIV. The velocity error in the mean flow of the examined hot jet flow with a maximal temperature of 191 °C does not result in a significant measurement uncertainty. However, it is unclear, whether in combustion flows with higher temperatures of one order of magnitude result in significant measurement uncertainty.

An indirect measurement of the resulting particle position errors inside a supersonic flow was performed by

the background-oriented Schlieren (BOS) technique with the assumption of a constant gradient of the refractive index in the line-of-sight direction of the camera in order to correct the resulting PIV measurement deviation of about 2-3 % (Elsinga et al., 2005). The standard BOS technique is a line-of-sight method and the resulting light deflection is integrated along the optical path through the refractive index field. Therefore, the standard BOS technique is only applicable to symmetric refractive index fields and has problems with asymmetric and turbulent fluctuations.
A qualitative measurement uncertainty analysis inside flame flows was conducted in (Stella et al., 2001) measuring the deflection of a light ray propagating through the flame for an estimation of the resulting image distortion. The deflection of the light rays mainly takes place in the flame front, where the highest temperature and hence refractive index gradients are located. Light sheet deflection leads to a curved measurement plane, but in combustion flows at laboratory scale the resulting PIV measurement uncertainty can be neglected. The measurement uncertainty caused by particle image distortion is mentioned to depend on the time interval between the laser pulses, but no quantitative information was given. It was assumed, that measurement errors only occur, if the flame front of the examined flame differs between the timely separated particle images. However, neither the movement of the particles inside the curved refractive index field nor the influence of the spatial shift between the measured velocity field to the real velocity field due to light deflection was discussed.
Additionally to the described uncertainty analysis methods, also the comparison with reference flow field measurements can be used for a quantification of measurement uncertainty due to refractive index fields, as it was performed for the influence of a turbulent propane gas flame and a glass plate contaminated with oil droplets (Schlüßler et al., 2014). However, only qualitative information about the resulting measurement uncertainty could be achieved for PIV measurements inside flames, because the measurement object was an air jet flow observed through the disturbing refractive index field.
Since only qualitative uncertainty estimations were performed for PIV measurements inside combustion flows, the present article provides a measurement technique for the quantification of resulting PIV measurement deviations inside flame flows. It is based on a direct measurement of the resulting position error in the PIV images by measuring the position of a glass rod tip inserted into the flame. The difference between the known position of the glass tip and the measured position is approximately the particle position error. Error propagation yields the resulting PIV measurement error inside the flame. The technique is applied to a premixed propane flame as an example. The measurement principle is described in section 2 and the measurement setup is depicted in section 3. The measurement results of performed PIV measurements inside the flame flow and the estimated systematic and random velocity errors are outlined in section 4.

2 Measurement principle

PIV measurements inside combustion flows are disturbed by a time dependent inhomogeneous refractive index field $n(\vec{r},t)$ with $\vec{r} = (x,y,z)^{\mathrm{T}}$, which causes image blurring and measurement errors of the particle positions. The light deflection of the scattered light on its path from a particle to the camera results in a detection of a particle actually positioned at $\vec{r_{\mathrm{P}}} = (x_{\mathrm{P}}, y_{\mathrm{P}}, z_{\mathrm{P}})^{\mathrm{T}}$ at a false position $\vec{r_{\mathrm{P'}}} = (x_{\mathrm{P'}}, y_{\mathrm{P'}}, z_{\mathrm{P}})^{\mathrm{T}}$ in the light sheet plane at (x,y,z_{P}). In premixed flames, the resulting particle position error $\vec{\xi} = \vec{r_{\mathrm{P'}}} - \vec{r_{\mathrm{P}}}$ is mainly caused by temperature gradients located in the region of the flame front (Stella et al., 2001). In order to determine the particle position error $\vec{\xi}$, a direct measurement of the light deflections is performed, whereby the known position of a glass rod tip is measured inside a flame by a camera. The difference between the measured position of the glass tip $\vec{r}_{\mathrm{G'}}$ and the known position $\vec{r}_{\mathrm{G}}$ is approximately the particle position error $\vec{\xi} = \vec{r_{\mathrm{P'}}} - \vec{r_{\mathrm{P}}} \approx \vec{r_{\mathrm{G'}}} - \vec{r_{\mathrm{G}}}$, cf. Fig. 1(a). It is assumed, that the insertion of a glass rod into the flame does not significantly affect the refractive index field on the optical path from the glass tip to the camera. A statistical analysis is finally performed to determine the mean particle position error $\overline{\vec{\xi}}$ and the standard deviation of the particle position error $\sigma_{\vec{\xi}}$.

3 Experimental setup

In this section, the experimental setups of the position error measurement technique and the PIV measurements are described. The setup of the direct measurement of the position error inside a premixed propane flame, which properties are described in section 3.1, is presented in section 3.2. The setup of the PIV measurements is described in 3.3.

3.1 Measurement object

The measurement object is a premixed propane flame. The schematic of the burner with a radial symmetric outlet and the examined flame is shown in Fig. 1(b) and (c). The premixing chamber of the burner is filled with spheres (ø= 5 mm), which homogenize the flow to prevent unintended flow characteristics in the burner outlet. The gas composition is set by a propane ($1\,\mathrm{L\,min^{-1}}$) and an air ($10\,\mathrm{L\,min^{-1}}$) inflow resulting in an equivalence ratio of $\phi = 2.4$. The burner outlet consists of a pipe with a diameter of 41.8 mm and a length of 300 mm. It provides a laminar flow condition. The resulting flame tends to fluctuate particularly in the diffusive region of the flame, cf. Fig. 1(c). These fluctuations can be explained by buyoancy effects (Nogenmyr et al., 2010).

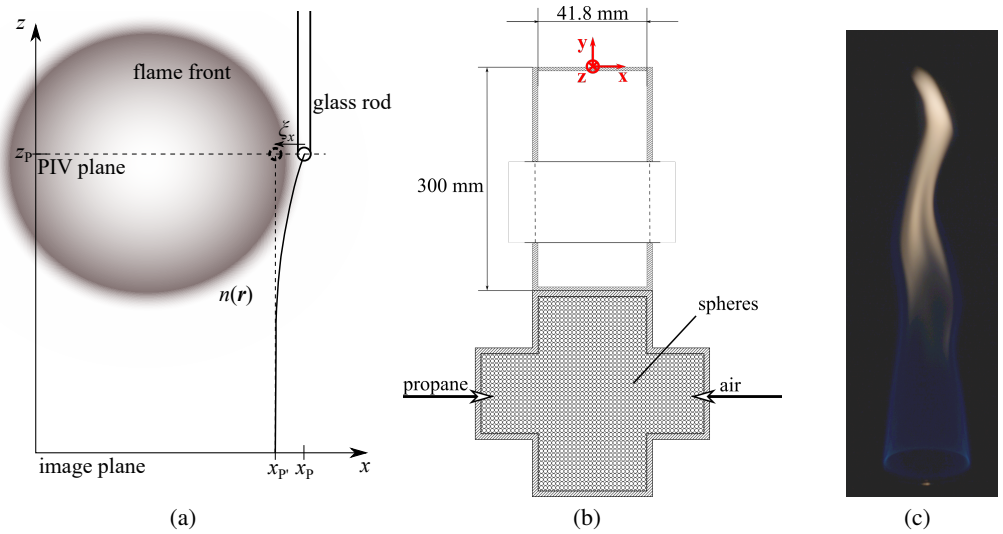

Figure 1: (a) Particle position error ξ_x in x-direction caused by light deflection of the scattered light from the glass rod in the PIV plane at $z = z_P$ to the camera in the image plane. In premixed flames, the refractive index field is mainly caused by the temperature field located in the flame front. (b) Schematic illustration of the burner with the sphere filled mixing chamber. (c) Flame for a propane inflow of $1\,\mathrm{L\,min^{-1}}$ and an air inflow of $10\,\mathrm{L\,min^{-1}}$.

3.2 Measurement of the position error

The resulting measurement error $\vec{\xi}(\vec{r})$ of the particle position is measured in three measurement planes M1, M2 and M3, illustrated in Fig. 2(a), which are perpendicular to the z-axis. M1 is located in the center of the burner outlet containing the symmetry axis, and M2 and M3 are located $z = 3$ mm and $z = 6$ mm parallel to M1 in viewing direction $\vec{k}$ of the camera, respectively. The measurement planes M2 and M3 are chosen in order to analyze the influence of the distance from the particles to the camera with respect to the refractive index field on the PIV measurement errors $\Delta\vec{v}$. The expected increase of the particle position error $\vec{\xi}$ with respect to the more distant measurement planes M2 and M3, cf. Fig. 2(a), will have an effect on the PIV measurement error $\Delta\vec{v}$, which is determined in this article. For this purpose, the known position of a glass rod tip with a diameter of 1.3 mm, which is inserted into the flame from the opposite of the camera viewing direction, cf. Fig. 2(b). Compared to the typical particle size in PIV measurements of a few micrometers, the glass rod diameter is three orders of magnitude larger, which leads to an averaging effect. Thus, the measured position error inside the flame is spatially low pass filtered, which leads to an underestimation of the occurring position errors.

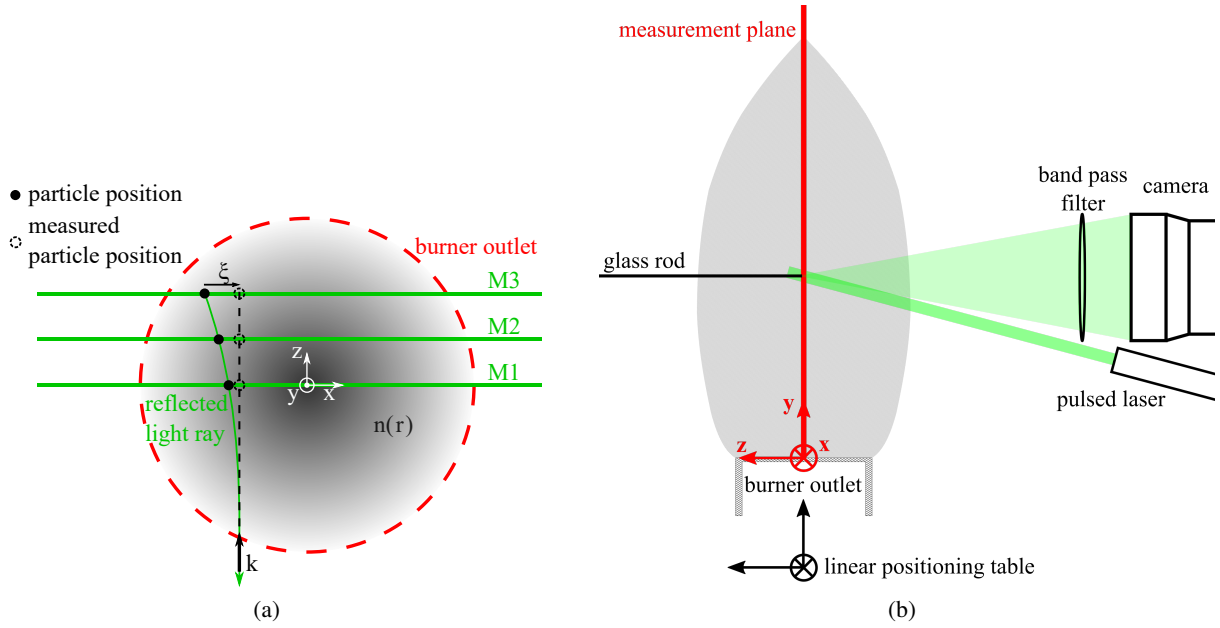

Figure 2: (a) Schematic illustration of the PIV measurement planes M1, M2 and M3 in top view of the burner outlet. (b) Schematic of the measurement setup for the position error $\vec{\xi}$.

By a relative movement of the burner with a positioning table, the position dependent error $\vec{\xi}(\vec{r})$ of the glass tip position is determined, assuming that the refractive index field in the optical path from the glass tip to the camera is not significantly disturbed by the glass rod. Using laser illumination with the laser wavelength (532 nm) as it is used in the PIV measurements and a band pass filter with a center wavelength of 532 nm at the camera prevent deviations due to dispersion. In addition, light emissions of the flame are filtered. Further, a laser pulse width of 1 ns results in a negligible time averaging. The cross-sensitivity of a possible bending of the glass rod due to flow forces is negligible. This was tested by the measurement of the glass tip position in an air flow with a higher volume flow compared to the combined propane and air flow of the flame. The material selection of the rod is decisive for the feasibility and accuracy of the measurement. First of all, the material must withstand the high temperatures of the flame and be inert in order not to corrode. Furthermore, the rod is not allowed to bend significantly. Quartz glass meets these requirements.

3.3 PIV measurement setup

The velocity field $\vec{v}(\vec{r})$ of the flame is measured by PIV in the three measurement planes M1, M2 and M3, cf. Fig. 2(a).The laser light sheet illumination (thickness 0.5 mm) is implemented by a dual pulse laser with 200 mJ pulse energy and a pulse length of less than 10 ns (Quantel Evergreen). The flow is seeded by titanium dioxide particles with a mean diameter of 0.4 µm. For observation, a 5.5 Mpx sCMOS camera (Andor Zyla) is positioned at $z = -60$ cm viewing in the positive z-direction with a 50 mm focal length objective (Zeiss Planar T* 1,4/50).

4 Results

In this section, the measurement results are described, starting in section 4.1 with the measured position error $\vec{\xi}(\vec{r})$ in the planes M1, M2 and M3. In section 4.2, the associated velocity fields $\vec{v}(\vec{r})$ measured with PIV are depicted. The resulting systematic and random velocity errors $\Delta\vec{v}(\vec{r})$ and $\sigma_{\Delta v}(\vec{r})$ of the PIV measurements are calculated in sections 4.3 and 4.4, respectively. As the velocity errors show only significant values in x-direction, the results are depicted only for the x-component.

4.1 Position error measurement

The velocity error $\Delta\vec{v}(\vec{r})$ of the PIV measurements is quantified by means of the position error $\vec{\xi}$ measured by the glass rod with

$$\frac{\Delta v_i}{v_i} = \nabla_i \xi_i - \frac{\nabla_i v_i}{v_i} \xi_i, \tag{1}$$

which is provided by Elsinga et al. (Elsinga et al., 2005). Here, $i = x, y, z$ denotes the component in the x, y or z-direction. Fig. 3 illustrates the mean position errors $\overline{\xi}_x$ in x-direction of the glass tip position in the considered measurement planes M1, M2 and M3 averaged over 500 single measurements. A two dimensional Gaussian filter with a standard deviation of 1.6 mm is applied to reduce the noise. The resulting position error inside the flame can be qualitatively explained by the temperature distribution, which is the dominating source of the refractive index field in premixed flames (Stella et al., 2001) and has its maximum in the flame front. The temperature distribution results in a density variation of the medium, which gives rise to a refractive index change. The connection between the density and the refractive index field is described by the Gladstone-Dale relation. Thus, high position errors occur in the region at $x \approx \pm 25$ mm in Fig. 3, where high temperature gradients are located between the flame front and ambient air at room temperature. Inside the flame, the temperature gradients are inverted due to the internal premixed gas flow at about room temperature. Therefore, in the lower part of the flame at $y < 40$ mm, where the internal unburned premixed gas flow exists, there are local extrema at $x \approx \pm 18$ mm in Fig. 3.

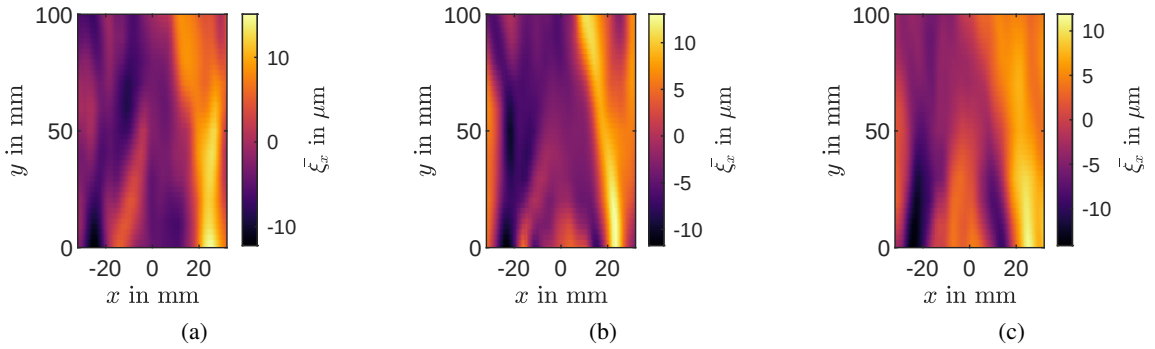

Figure 3: Measured particle position error $\overline{\xi}_x$ in the planes M1 (a), M2 (b) and M3 (c).

4.2 PIV measurement results

Fig. 4 shows the mean velocity field $\overline{\vec{v}}(\vec{r})$ of 500 single PIV measurements captured with 15 Hz repetition rate with a time separation between the laser pulses of 400 µs and the corresponding standard deviation of the x-component of the velocity σ_{v_x} in the measurement planes M1, M2 and M3. The maximal velocity amounts up to 0.24 m s^{-1} and is located around the flame front, which exhibits a conical shape. The maximal standard deviation of the x-component of the velocity σ_{v_x} is located in the bright diffusive region of the flame, where the flame tends to fluctuate, and amounts up to about 0.1 m s^{-1}, cf. Fig. 1(c). The mean flow velocity shows a minor clockwise tilted direction, which leads to a slightly skewed symmetry axis.

4.3 Systematic velocity error

The relative systematic velocity error $\frac{\overline{\Delta v_i}}{\overline{v}_i}$ is determined by the insertion of the mean position error $\overline{\xi}_i$ and the mean velocity $\overline{v}_i$ in Eq. (1). The particle position errors $\overline{\xi}_x(\vec{r})$ and the velocity fields $\vec{v}(\vec{r})$ in the planes M1, M2 and M3 inside the combustion flow were measured with a glass rod and with PIV, respectively. With Eq. (1), an estimation of the systematic velocity error inside the flame flow is performed and the resulting systematic measurement error of the mean velocity field standardized to the mean velocity of the entire flow $\tilde{v}_x$ is depicted in Fig. 5. The highest 1 % of the resulting systematic velocity error values are truncated

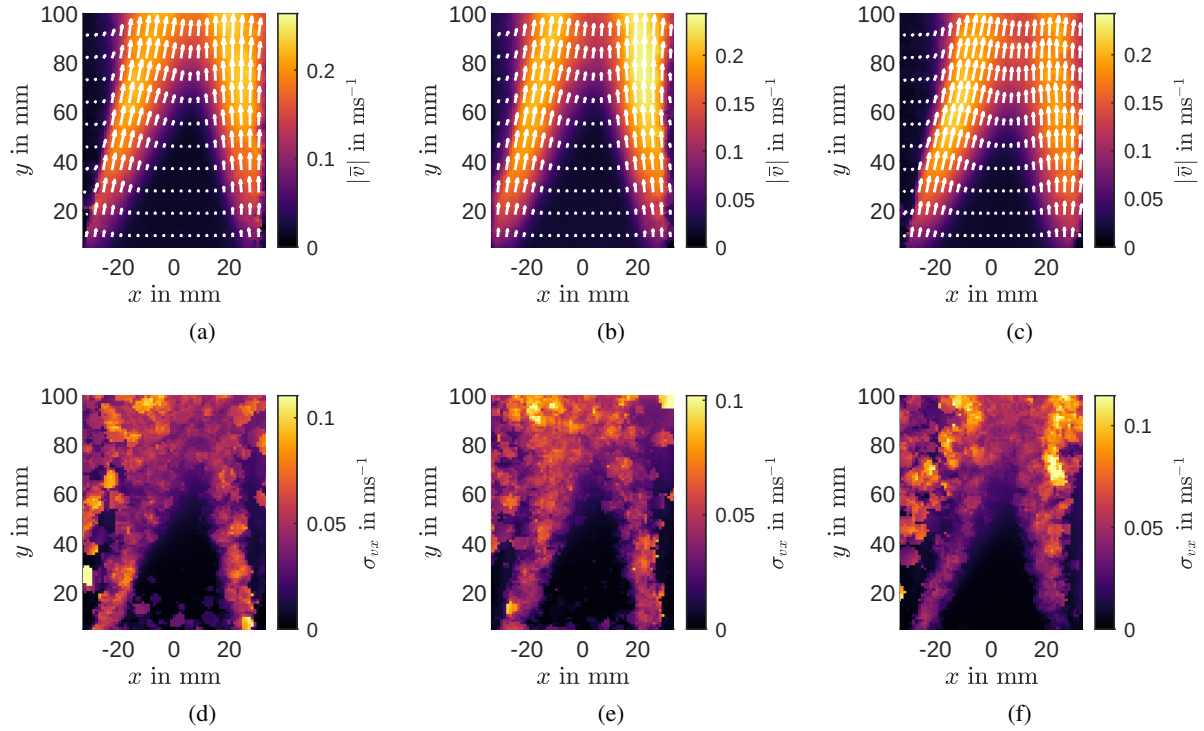

Figure 4: Measured mean velocity field of 500 single measurements in the planes M1 (a), M2 (b) and M3 (c) and the corresponding standard deviation of the x-component of the velocity σ_{v_x} (d) to (f).

in order to ignore outliers. The maxima are located around the flame front, where the velocity gradients $\nabla_x \overline{v}_x$, the particle position error $\overline{\xi}_x$ and its gradient $\nabla_x \overline{\xi}_x$ show high values. The reduction of the maximal systematic error regarding the measurement planes M2 and M3 seems to be counterintuitive, because the propagation distance of the reflected light inside the refractive index field increases. Though, the reduction of the systematic error can be explained by the light paths inside the refractive index field. The reflected light of the particles or rather the glass rod tip is spatially filtered by the spatial angle of the aperture of the camera objective. So diverging light rays from the object are detected and consequently, the light rays are affected by different refractive index values resulting in a spatial filter of the affecting refractive index field. The spatial filter smooths the refractive index edge at the border of the flame front and reduces the occurring systematic velocity error. However, it can also be assumed, that the particle images appear blurred and thus, the signal to noise ratio will be reduced. Anyway, systematic velocity errors of at least 3 % to 4.5 % occur in the examined measurement planes inside the flame. Hence, compared to the typical PIV measurement uncertainty of about $1-2\,\%$ (Westerweel, 1997; Voges et al., 2007), the effect of light refraction inside flame flows due to refractive index fields can lead to significant systematic measurement errors in the region around the flame front. This region is also of particular interest for studying the dynamics of combustion chemistry (Kiefer et al., 2008; Schlüßler et al., 2015), which requires high precision and reliable velocity data. In order to achieve that, the accuracy of the velocity data can be improved by the correction of the velocity error calculated with the presented method, which is depicted in Fig. 5.

4.4 Random velocity error

As the systematic velocity error is quantified by Eq. (1), the error propagation of Eq. (1) is used to estimate random velocity errors, which is justified with the assumption that the fluctuating refractive index field is

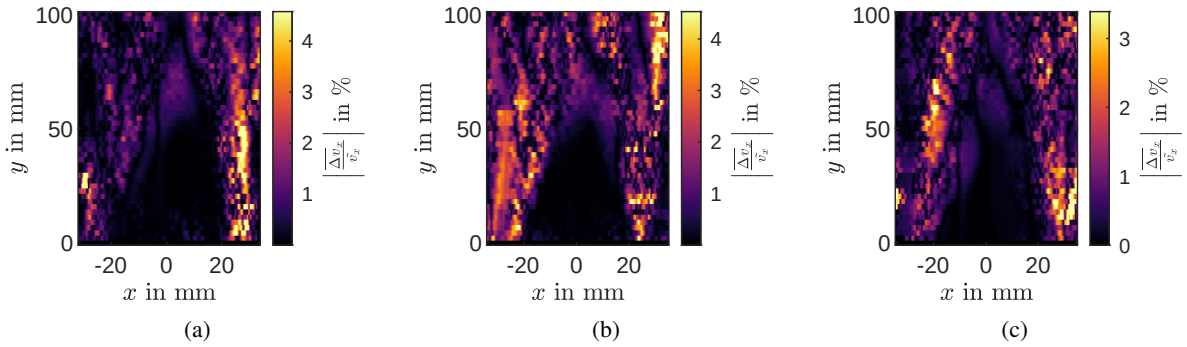

Figure 5: Relative systematic measurement error $\left|\frac{\overline{\Delta v_x}}{\tilde{v}_x}\right|$ of the PIV measurement caused by particle position error in the planes M1 (a), M2 (b) and M3 (c).

the dominant source of the random position error

$$\sigma_{\Delta v_i} = \sqrt{\left(\frac{\partial \Delta v_i}{\partial \xi_i}\sigma_{\xi_i}\right)^2 + \left(\frac{\partial \Delta v_i}{\partial v_i}\sigma_{v_i}\right)^2 + 2\frac{\partial}{\partial \xi_i}\frac{\partial}{\partial v_i}\mathrm{cov}\left(\xi_i, v_i\right)}$$
$$\approx \sqrt{\left(\nabla v_i \sigma_{\xi_i}\right)^2 + \left(\nabla \xi_i \sigma_{v_i}\right)^2}. \tag{2}$$

Here, $\sigma_{\Delta v_i}$, σ_{ξ_i} and σ_{v_i} are the standard deviations of Δv_i, ξ_i and v_i, respectively and $\mathrm{cov}\left(\xi_i, v_i\right)$ is the covariance of ξ_i and v_i. A positive covariance term can be expected, due to the fact, that high velocities and high particle position errors are located in the flame front. Further, the formation mechanism of increased velocity and increased light refraction arise from the heating of the fluid, which leads to expansion and convection, and a reduction of the local density varying the refractive index. Moreover, it is assumed, that the covariance term is much smaller than the first and second term due to the fact that the velocity field is measured inside the PIV measurement plane and the particle position error arise from the refractive index field on the optical path from the measurement plane to the camera. Therefore, a lower limit of the actual random error is estimated, resulting in a best case scenario. The resulting random measurement error is standardized to the mean velocity of the entire flow $\tilde{v}_x$ in x-direction and is depicted in Fig. 6. Again, the highest 1 % of the resulting systematic velocity error values are truncated in order to ignore outliers. Like the maximal systematic errors, also the maximal random velocity errors are located in the region around the flame front. However, compared to the systematic measurement errors, the random measurement errors vary more intense in the examined measurement planes with a maximum of about 9 %.
As the quantified systematic and random errors are estimated by the particle position error, one could counter, that an additional averaging effect will result by the interrogation window of the PIV evaluation algorithm. Though, the measured particle position error already includes an averaging effect by the 1.3 mm diameter of the glass rod resulting in a measurement area of about 1.3 mm^2. Considering an interrogation window of 16×16 px^2 and an image size of one pixel of 10 µm, the resulting measurement area is 0.03 mm^2. Thus, the averaging affect of the interrogation window is overcompensated within the measurement setup.

5 Conclusion

The measurement error of the particle position in PIV measurements due to inhomogeneous refractive index fields inside combustion flows leads to velocity measurement errors, which are generally unknown. We propose an experimental method providing quantitative information about occurring PIV measurement errors inside flame flows. A velocity field of a premixed propane flame flow is taken as an example. Resulting position errors inside the measurement plane due to light refraction are determined experimentally. The experimental approach is based on the position measurement of a glass rod tip inserted into the flame. Based on the measured position error, the resulting velocity errors of performed PIV measurements are determined.

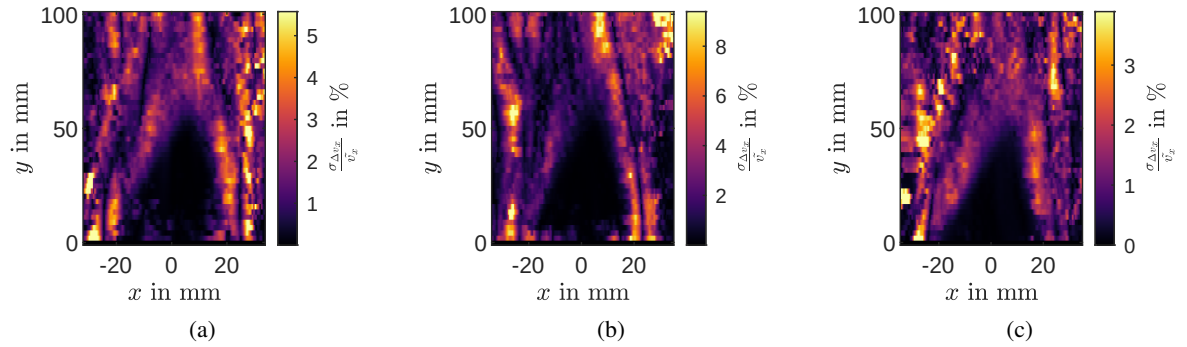

Figure 6: Relative random measurement error $\frac{\sigma_{\Delta v_x}}{\bar{v}_x}$ of the PIV measurement caused by particle position error in the planes M1 (a), M2 (b) and M3 (c).

As the measurement error of the particle position depends on the distance of the scattering light path between the particles and the camera, the position error was determined in three different measurement planes located at the center of the flame flow and 3 mm and 6 mm behind the center of the flow with respect to the viewing direction of the camera. The resulting maximal relative systematic measurement errors were found to be 3 % to 4.5 % for the examined measurement planes. A significant increase of the systematic measurement errors with respect to a 6 mm increased optical path length inside the refractive index field of the flame was not observed. The random measurement errors were estimated by means of error propagation of the measured position error and the measured velocity, which results in a maximal relative random velocity error between 4 % and 9 %. Moreover, the random error appears to be more sensitive with respect to the optical paths within the inhomogeneous refractive index field. It shall be mentioned, that the resulting measurement errors are sensitive to the dimension of the examined flame or rather the inhomogeneous refractive index field. Besides the optical path length inside the refractive index field, also the maximal temperatures, the mixing ratio between the fuel and oxidant as well as the used fuel influence the refractive index. Thus, all these parameters affect the resulting measurement errors. The estimated PIV measurement errors, therefore, have to be considered individually for various measurement setups. In conclusion, the systematic as well as the random measurement errors can significantly affect the PIV measurement inside flame flows, where the largest measurement errors occur in the region of the flame front. So, for precise measurements inside larger flame flows, the measurement uncertainty due to light refraction is problematic and should be taken into account. This is particularly important when the experimental data are used to validate results from numerical simulations (Barlow, 2007), e.g by Reynolds-averaged Navier Stokes (RANS) or large eddy simulations (LES). The presented method provides a tool for the determination of the PIV measurement uncertainty.

References

Barlow RS (2007) Laser diagnostics and their interplay with computations to understand turbulent combustion. *Proceedings of the Combustion Institute* 31:49–75

Elsinga GE, van Oudheusden BW, and Scarano F (2005) Evaluation of aero-optical distortion effects in PIV. *Experiments in Fluids* 39:246–256

Fischer A (2016) Fundamental uncertainty limit of optical flow velocimetry according to Heisenberg's uncertainty principle. *Applied Optics* 55:8787

Fischer A (2017) Imaging Flow Velocimetry with Laser Mie Scattering. *Applied Sciences* 7:1298

Kiefer J, Li ZS, Zetterberg J, Bai XS, and Aldén M (2008) Investigation of local flame structures and statistics in partially premixed turbulent jet flames using simultaneous single-shot CH and OH planar laser-induced fluorescence imaging. *Combustion and Flame* 154:802–818

Nobach H and Bodenschatz E (2009) Limitations of accuracy in PIV due to individual variations of particle image intensities. *Experiments in Fluids* 47:27–38

Nogenmyr KJ, Kiefer J, Li ZS, Bai XS, and Aldén M (2010) Numerical computations and optical diagnostics of unsteady partially premixed methane/air flames. *Combustion and Flame* 157:915–924

Schlüßler R, Bermuske M, Czarske J, and Fischer A (2015) Simultaneous three-component velocity measurements in a swirl-stabilized flame. *Experiments in Fluids* 56:183

Schlüßler R, Czarske J, and Fischer A (2014) Uncertainty of flow velocity measurements due to refractive index fluctuations. *Optics and Lasers in Engineering* 54:93–104

Steinberg AM, Boxx I, Stöhr M, Carter CD, and Meier W (2010) Flow flame interactions causing acoustically coupled heat release fluctuations in a thermo-acoustically unstable gas turbine model combustor. *Combustion and Flame* 157:2250–2266

Stella A, Guj G, Kompenhans J, Raffel M, and Richard H (2001) Application of particle image velocimetry to combusting flows: design considerations and uncertainty assessment. *Experiments in Fluids* 30:167–180

Vanselow C and Fischer A (2018) Influence of inhomogeneous refractive index fields on particle image velocimetry. *Optics and Lasers in Engineering* 107:221–230

Voges M, Beversdorff M, Willert C, and Krain H (2007) Application of particle image velocimetry to a transonic centrifugal compressor. *Experiments in Fluids* 43:371–384

Westerweel J (1997) Fundamentals of digital particle image velocimetry. *Measurement Science and Technology* 8:1379